Fidelity of *in Vitro* DNA Strand Transfer Reactions Catalyzed by HIV-1 Reverse Transcriptase†

James A. Peliska‡ and Stephen J. Benkovic*

Department of Chemistry, The Pennsylvania State University, 415 Wartik Laboratory, University Park, Pennsylvania 16802

Received November 4, 1993; Revised Manuscript Received January 14, 1994®

ABSTRACT: The fidelity of DNA strand transfer reactions catalyzed by human immunodeficiency virus type 1 reverse transcriptase has been studied *in vitro*. A model system involving two sequential DNA strand transfers was developed to simulate the process of forced copy-choice recombination. A propensity for nucleotide misincorporation at the junction of the strand transfer, as determined by DNA sequencing of the reaction products, was found consistent with a model involving the addition of nontemplate-directed nucleotides prior to the transfer of nascent DNA onto the accepting RNA template [Peliska, J. A., & Benkovic, S. J. (1992) *Science 258*, 1112]. The kinetic and mechanistic factors that may dictate which nucleotide bases are incorporated at recombination sites during strand transfer and the possible consequences of recombination-induced mutagenesis *in vivo* are discussed.

The diploid genome of retroviruses undergoes genetic variation at a very high rate. A number of processes are believed responsible, including nucleotide misincorporation during DNA synthesis (Bebenek & Kunkel, 1993; Bebenek et al., 1989; Roberts et al., 1988; Ji & Loeb, 1992; Preston et al., 1988; Mendelman et al., 1990; Ricchetti et al., 1990) and recombination (Temin, 1993) during the process of reverse transcription. A consequence of this genetic variation is the rapid occurrence of antibody- and drug-resistant strains of human immunodeficiency virus type 1 (HIV-1). Understanding the factors that contribute to this variation is critical to the design of effective antiviral agents.

One particular recombination event, entitled forced copy-choice recombination (Coffin, 1979; Hu et al., 1993), is thought to occur when the viral RNA genome has been damaged (Figure 1). In this case, minus strand DNA synthesis proceeds until a break in the viral RNA genome (template a) is encountered by the reverse transcriptase (RT). Guided by sequence homology between the diploid RNA strands, the growing DNA transfers onto the second RNA template (template b) and continues to synthesize DNA. We recently proposed (Peliska & Benkovic, 1992) that nucleotide misincorporation occurs during this process of forced copy-choice recombination based on the observation that upon encountering a break in the RNA template, HIV-1 RT catalyzes the addition of nontemplate-directed nucleotides onto the blunt end of the DNA·RNA duplex (Figure 1B, illustrated for an A mismatch). After DNA strand transfer onto the second RNA template, depending on the sequence of the RNA template, a mismatch may result. Since the RT lacks a proofreading exonuclease activity and is proficient in extending terminal base mismatches, the terminal mismatch is permanently incorporated upon DNA synthesis.

In this report, we describe *in vitro* experiments that confirm our proposed misincorporation model using an assay system involving two consecutive DNA strand transfers and oligonucleotide DNA sequencing techniques. Factors that could contribute to the frequency and distribution of incorporated nucleotides at strand transfer junctions are discussed.

MATERIALS AND METHODS

Materials. DNA oligonucleotide primers and runoff transcription template-primers were purchased from Midland Certified Reagent Co. All deoxy- and ribonucleotide triphosphates were from Pharmacia (Ultrapure). Molecular biology grade reagents, including acrylamide, $MgCl_2$, ammonium acetate, dithiothreitol, and EDTA, were purchased from Sigma. Radionucleotides were purchased from NEN. Sequenase reagents were from U.S. Biochemicals. Recombinant HIV-1 reverse transcriptase purified as a p66/p51 heterodimer according to Mizrahi et al. (1989) was a gift of Dr. Christine Debouck of SmithKline Beecham Pharmaceuticals. The active concentration of HIV-1 RT was determined by active-site titration using a modification of the method described by Reardon and Miller (1990). *Escherichia coli* strain BL21 carrying pAR1219 for the overexpression of T7 RNA polymerase was provided by Dr. F. W. Studier, and the protein was purified using a modification of published procedures (Grodberg & Dunn, 1988).

Oligonucleotide Substrates. RNA templates were synthesized by runoff transcription with T7 RNA polymerase (Milligan & Uhlenbeck, 1989). A trace quantity of [α-^{32}P]-UTP was included in the transcription reaction to facilitate the purification and quantitation of the RNA products. RNA was purified by electrophoresis through 20% acrylamide/8 M urea/TBE (90 mM Tris/64.6 mM boric acid/2.5 mM EDTA, pH 8.3), elution from the excised gel using 0.5 M ammonium acetate at 37 °C, and precipitation with ethanol. RNA samples were stored as ethanol suspensions at −70 °C until used.

DNA oligonucleotides were labeled at their 5′-end with T4 polynucleotide kinase using [γ-^{32}P]ATP according to the manufacturer's protocol (U.S. Biochemicals). After the reaction, the DNA was extracted twice with 1:1 phenol/chloroform and then with chloroform.

Double-Jump Strand Transfer Reactions. A 24-base DNA primer was annealed to 40-base RNA template 1 by mixing equal molar quantities and slow-cooling from 65 °C. The

† This was supported by National Institutes of Health Grant GM13306 (S.J.B.) and by NIH Fellowship Award AI08275 (J.A.P.).

* To whom correspondence should be addressed.

‡ Present address: Department of Biological Chemistry, University of Michigan, Ann Arbor, MI 48109-0606.

® Abstract published in *Advance ACS Abstracts,* March 1, 1994.

0006-2960/94/0433-3890$04.50/0

Scheme 1

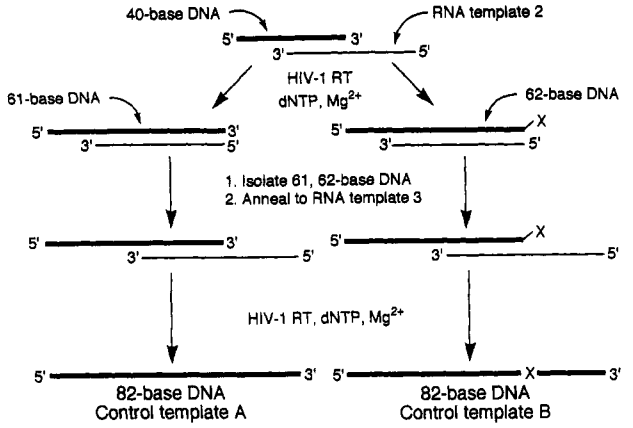

strand transfer was conducted in the presence of RT buffer (50 mM Tris-HCl, pH 8.0, 75 mM KCl, 0.1 mM EDTA, 1 mM dithiothreitol, and 0.1% Triton X-100), 100 μM each dNTP, 7 mM $MgCl_2$, 200 nM 24-base DNA·40-base RNA primer·template, 700 nM 41-base RNA template 2, 700 nM 42-base RNA template 3, and 100 nM HIV-1 RT in a final volume of 10 μL. When reaction products were to be sequenced, mixtures were incubated at 37 °C for 2 h. Reactions were terminated by the addition of 40 μL of H_2O and 2 μg/mL DNase-free RNase A with incubation at room temperature for 30 min. The terminated reaction was extracted with 50 μL of 1:1 phenol/chloroform followed by 50 μL of chloroform. The extract was subjected to two 1-mL spun columns (Sephadex G-25 in H_2O) and taken to dryness *in vacuo*.

Double-Jump DNA Sequencing. The dried DNA sample was dissolved in 7 μL of 50 mM Tris-HCl, pH 7.5, and hybridized to 5'-^{32}P-labeled 15-base DNA sequencing primer (100 nM) in Sequenase buffer (USB) by slow-cooling from 65 °C. This 5'-^{32}P-labeled 15-base DNA·82-base DNA primer·template DNA (5 μL) was added to a solution containing 7.7 mM DTT, 1× Sequenase buffer, and 80 μM of each dNTP. Sequencing reactions were initiated by addition of this mixture (3 μL) to 2 μL of ddNTP (60 μM in 50 mM NaCl) and 1 μL of Sequenase [stock diluted 1:16 with cold TE buffer (10 mM Tris-HCl/1 mM EDTA, pH 7.5)]. This reaction was performed for each ddNTP. Mixtures were incubated at 37 °C for 3 min and then quenched by the addition of 5 μL of 20 mM EDTA in 90% formamide/TBE. Samples were subjected to electrophoresis through a 20% acrylamide/8 M urea/TBE gel. The gel was exposed to a Molecular Dynamics Phosphorimage screen, and the image was analyzed on a Molecular Dynamics Phosphorimager.

Synthesis of Control Template. The synthesis of the sequencing control template is outlined in Scheme 1. A control template devoid of mutations was synthesized by a stepwise purification of DNA transfer products. A sample of 40-base DNA (primary DNA product of RNA template 1) was 5'-^{32}P-labeled to low specific activity (~850 cpm/pmol) and hybridized to 41-base RNA template 2. This template·primer (500 nM) was extended by the addition of HIV-1 RT (200 nM), RT buffer, $MgCl_2$ (7 mM), and each dNTP (100 μM each). The reaction mixture was incubated at 37 °C for 2.5 min and then quenched with 90% formamide/TE containing 20 mM EDTA. The quenched sample was then subjected to electrophoresis through 20% acrylamdie/8 M urea/TBE until the xylene cyanol F dye ran off the gel bottom. The resulting gel was exposed to film overnight at −70 °C. The 61-base DNA product was located, the gel excised, and the DNA eluted with 0.5 M ammonium acetate at 37 °C over 5 h. The observed 62-base DNA blunt-end addition products was also isolated for sequencing (control template B). The eluted DNA was concentrated, ethanol-precipitated, and dissolved in 100 μL of H_2O. The sample was further desalted by passage through one 1-mL spun column (Sephadex G-25), dried *in vacuo*, and dissolved in 50 mM Tris-HCl, pH 7.5.

The resulting 61-base DNA and 62-base DNA were then annealed to 42-base RNA template 3. These hybrids were elongated by HIV-1 RT as described above to produce the 82-base DNA strand subject to sequencing.

Strand transfer and sequencing reactions were performed at least 3 times with essentially identical results.

RESULTS AND DISCUSSION

In this report, we describe experiments designed to determine (1) if misincorporations result at the point of recombination as predicted by the model in Figure 1 and (2) what factors may be involved in selecting bases for preferential incorporation at the recombination site. To address these points, a two-jump strand transfer assay was developed wherein HIV-1 RT is required to undergo two sequential DNA strand transfer reactions (Figure 2). To accomplish this, three RNA templates are utilized, each with overlapping sequence homology. The product of the first DNA strand transfer reaction is a 61-base DNA product. A subsequent second DNA strand transfer gives rise to an 82-base DNA product. The DNA product of the two-jump transfer is shown in Figure 2 along with the expected sites of recombination-induced misincorporation based on the model shown in Figure 1B.

Figure 3 illustrates the time course of the double-jump strand transfer showing the substrate dependencies for each strand transfer event. In the absence of RNA template 3 necessary for the second DNA strand transfer (Figure 2), 61-base DNA product accumulates, but no 82-base product indicative of a second strand transfer event is observed (Figure 3A, left panel). When RNA template 3 is included in the assay while RNA template 2 is omitted, no strand transfer is observed, and only 40-base DNA resulting from synthesis to the end of RNA template 1 occurs (Figure 3A, middle panel). This result demonstrates the specificity of the strand transfer event since RNA template 3 cannot support DNA strand transfer in the absence of RNA template 2. Only in the presence of all three RNA templates does the 82-base DNA product derived from two-strand transfer events accumulate. A significant amount of apparent blunt-end addition product is observable at both jump sites. The nature of the weak intermediate bands between the 61-base and 82-base products in the reaction containing both 41-base and 42-base RNA templates was not examined but probably represent polymerase pause sites. They do not appear to represent blunt-end addition products since they are not observed in the control reaction lacking the 42-base RNA template (Figure 3, left panel).

The time course of 61-base DNA (product of the first strand transfer) and 82-base DNA (product of the second strand transfer) production is shown in Figure 3B. The lag in strand transfer product has been attributed to a rate-limiting process involving HIV-1 RT RNase H mediated removal of RNA fragments annealed to the nascent DNA strand before transfer onto the accepting RNA template (Peliska & Benkovic, 1992). Interestingly, after the initial lag period of the reaction, the rate of 82-base DNA (second strand transfer) production equals that of the 61-base product (first strand transfer). Thus, even at relatively low concentrations of 61-base DNA product

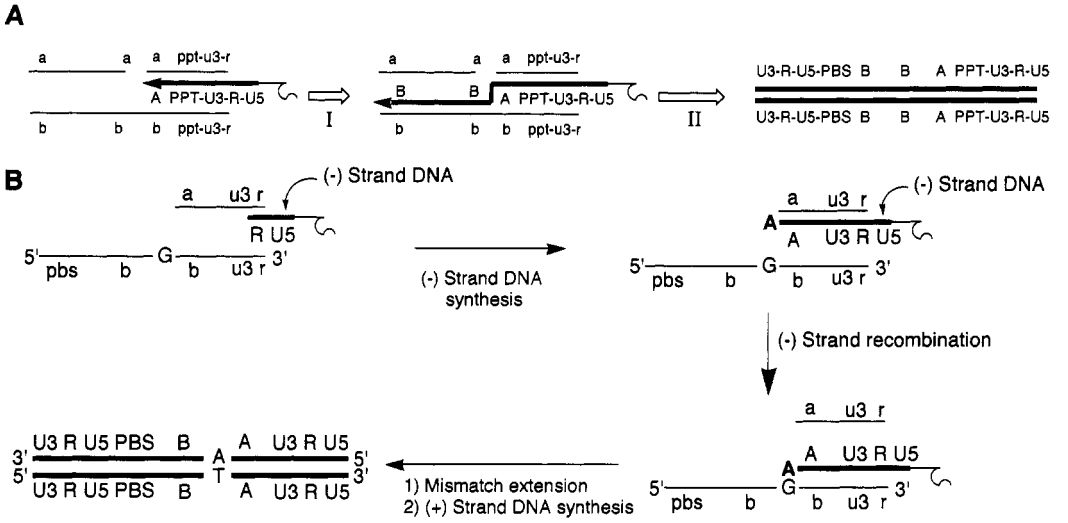

FIGURE 1: (A) Forced copy-choice recombination. During reverse transcription, DNA synthesis (boldface lines, uppercase letters) proceeds using retroviral RNA as template (thin lines, lowercase letters). If a break in the RNA is encountered, the DNA is transferred onto the second RNA template (b), and DNA synthesis continues. (B) Model for misincorporation during forced copy-choice recombination. As in (A), the RT synthesizes DNA until encountering a break in the RNA template (a). Before the nascent DNA is transferred onto the second RNA template (b), RT adds an additional base (shown here as dAMP) onto the blunt end of the DNA·RNA intermediate. After DNA transfer onto the second RNA template, a mispair could result (shown here as a G-A mispair). Extension of the mismatch results in base conversion upon synthesis of plus strand DNA. Symbols: PBS, tRNA primer binding site; ppt, polypurine tract; u3 and U3, unique 3′ sequences; u5 and U5, unique 5′ sequences; r and R, repeat sequences.

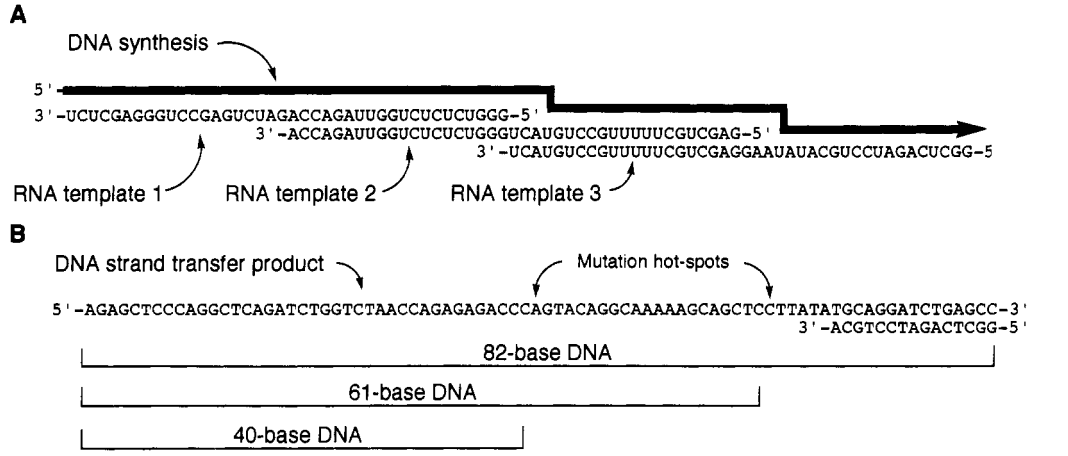

FIGURE 2: Strand transfer assay. (A) Three templates are utilized in the two-jump DNA strand transfer assay. The sequences of the three RNA templates are shown with their overlapping sequence homologies. The direction of DNA synthesis is shown by the boldface arrow. The first strand transfer generates a 61-base DNA product, and the subsequent transfer gives rise to a 82-base full-length product. (B) The 82-base DNA product generated by the two-jump strand transfer assay shown in (A). The expected sites of sequence variation based on the model in Figure 1B are shown along with the intermediate strand transfer product lengths and the 15-base DNA primer used in sequencing the DNA product.

(a 40-base DNA:61-base DNA ratio of approximately 7:1 at 10 min), the second strand transfer catalyzed by HIV-1 RT proceeds at a rate comparable to the first strand transfer. This is consistent with the proposed associative mechaism of DNA strand tranfer catalyzed by HIV RT wherein the acceptor RNA strand and the nascent DNA strand begin hybridization before completion of the strand transfer event (Peliska & Benkovic, 1992). In such a mechanism, the concentration dependence for the DNA substrate is largely removed since transfer occurs from an enzyme-bound intermediate. Further kinetic data are required to confirm this possibility.

The question of fidelity during DNA strand transfer was addressed by sequencing the 82-base DNA product. To accomplish this, a 15-base sequencing primer was designed to complement the 3′-end bases of the 82-base DNA product. Since this primer is specific for only full-length DNA product resulting from both strand transfer reactions, interference from smaller DNA fragments is avoided. The DNA products were sequenced directly using the dideoxynucleotide method with elevated concentrations of ddNTP to accommodate the short length of DNA. Since the transfer products were sequenced directly, sequence artifacts resulting from DNA amplification or selection were avoided. On the basis of the misincorporation model presented in Figure 1, a distribution of sequencing bands at the site(s) of recombination is expected. Figure 4 shows that a distribution of DNA sequences is present at both jump sites at positions consistent with the model presented in Figures 1 and 2. At the position of the first DNA strand transfer, a control template devoid of DNA mutations shows the expected sequence surrounding the transfer site. The template resulting from a strand transfer reaction clearly shows a distribution of all four possible nucleotide sequences at the first nucleotide beyond the strand transfer junction. In accord with earlier predictions (Peliska & Benkovic, 1992) a significant number of strand transfers resulted in misincorporation at the transfer

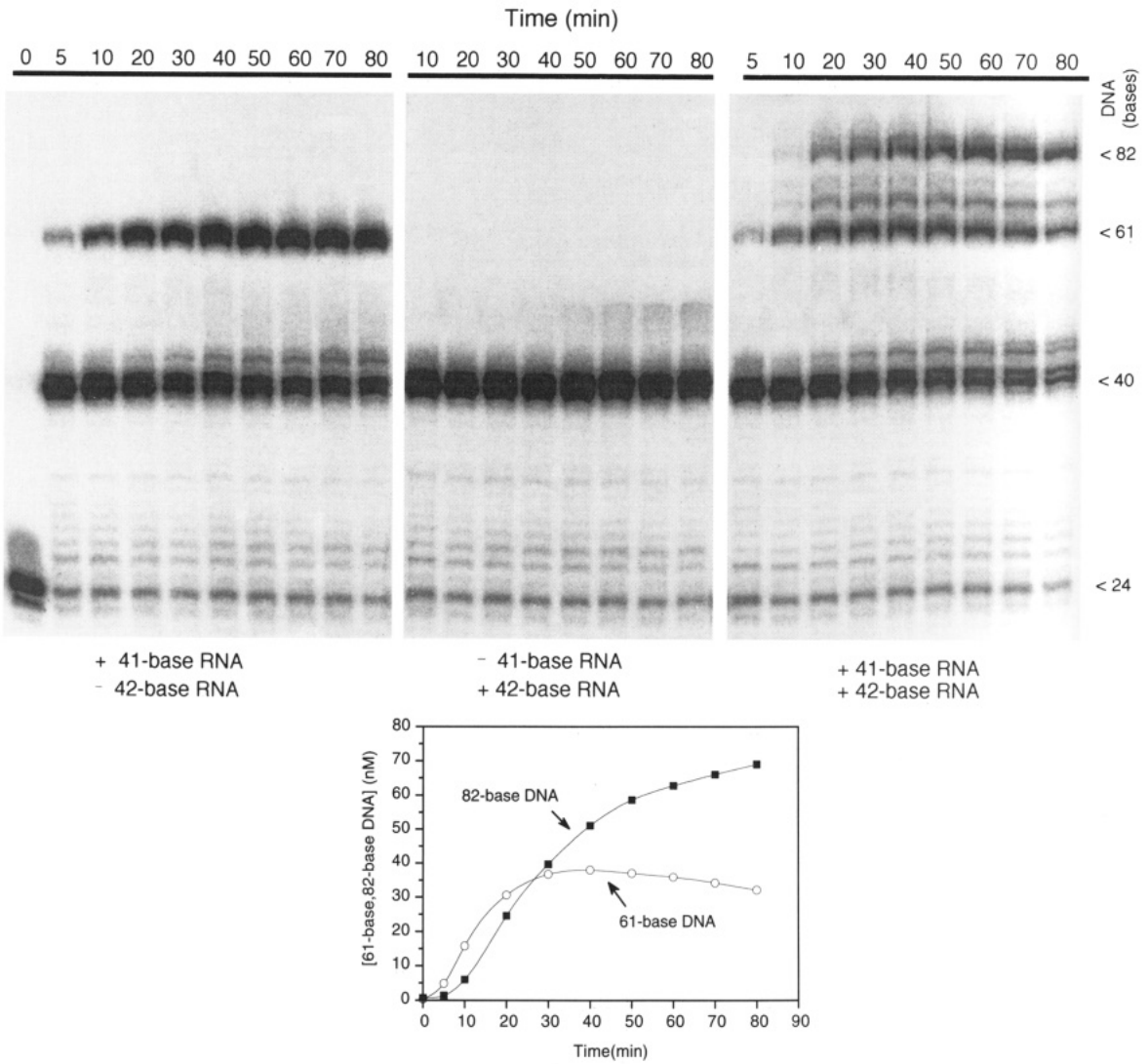

FIGURE 3: Specificity of the DNA strand transfer assay. (Top panel, A) Each reaction contained 200 nM 5′-^{32}P-labeled 24-base DNA·40-base RNA template 1, 100 nM HIV-1 RT, 7 mM $MgCl_2$, and 100 μM each dNTP in RT buffer at 37 °C. Left panel: reaction also contained 700 nM 41-base RNA template 2. Middle panel: reaction contained 700 nM 42-base RNA template 3. Right panel: reaction contained 700 nM 41-base RNA template 2 and 700 nM 42-base RNA template 3. At the time indicated, reaction samples were quenched with EDTA and then subjected to PAGE. The lengths of the DNA products are shown at the right. (Bottom panel, B) Time course of the reaction in (A), right panel. The production of 61-base DNA product (resulting from the first strand transfer) and 82-base DNA (resulting from the second strand transfer) is shown as a function of time. Products were quantitated using ImageQuant software (Molecular Dynamics). Concentrations were determined based on the fraction of turnover to product and the total substrate concentration in the reaction mixture.

junction. While detailed quantitative arguments are not possible using this sequencing technique, it does appear that the correct nucleotide dAMP (sequenced as T) was preferentially inserted at the first jump site during reverse transcription. Previous studies had shown that the efficiencies of blunt-end addition onto the end of the transfer intermediate differ for the four dNTP substrates (Peliska & Benkovic, 1992). Under those conditions, the rates of blunt-end addition followed the order dATP (1) > dGTP (0.5) > dTTP (0.2) > dCTP (0.07). The observed sequence distribution observed in Figure 4 does not appear to follow this trend strictly since dCMP (sequenced as G) is expected to be incorporated at very low levels, but in the strand transfer reactions is found in equal or possibly even higher levels than both dGMP and dTMP. As anticipated, dAMP (sequenced as T) is preferentially incorporated as observed in control template B.

Examination of the sequences surrounding the second strand transfer reveals similar sequence discrepancies. The sequence of the control template derived from the purified 61-base DNA intermediate (Scheme 1) shows the expected band due to the correct incorporation of dCMP (sequenced as G) along with faint bands due to premature polymerase termination during sequencing.[1] The sequence of the control template derived from purified 62-base DNA (single-base blunt-end addition) (Scheme 1) suggests that blunt-end addition follows a preference similar to that seen for the first strand transfer site. Indeed, dTMP appears to be the major sequence detected at this site, representing a blunt-end addition of a dAMP. A high level of dCMP blunt-end addition (sequenced as G) is

[1] Attempts to eliminate the anomalous sequence band artifacts around the second jump site were unsuccessful. This is due to the length of the sequenced oligonucleotide and the short distance of the jump site from the sequencing primer (5–6 bases) resulting in some Sequenase termination products. The upper bands of the "split" bands at the second transfer site represent anomalous sequencing termination products while the lower bands represent the misincorporated base sequence at this site. Short oligonucleotides often show slight sequence-dependent changes in electrophoretic mobility, and the high resolution of the 20% acylamide gels used in the sequence determination exaggerates this characteristic. However, the intensity of the bands in the control template versus strand transfer reactions is well above this background. Since each experiment was done multiple times with the same observed results, the qualitative interpretations discussed in the text are valid.

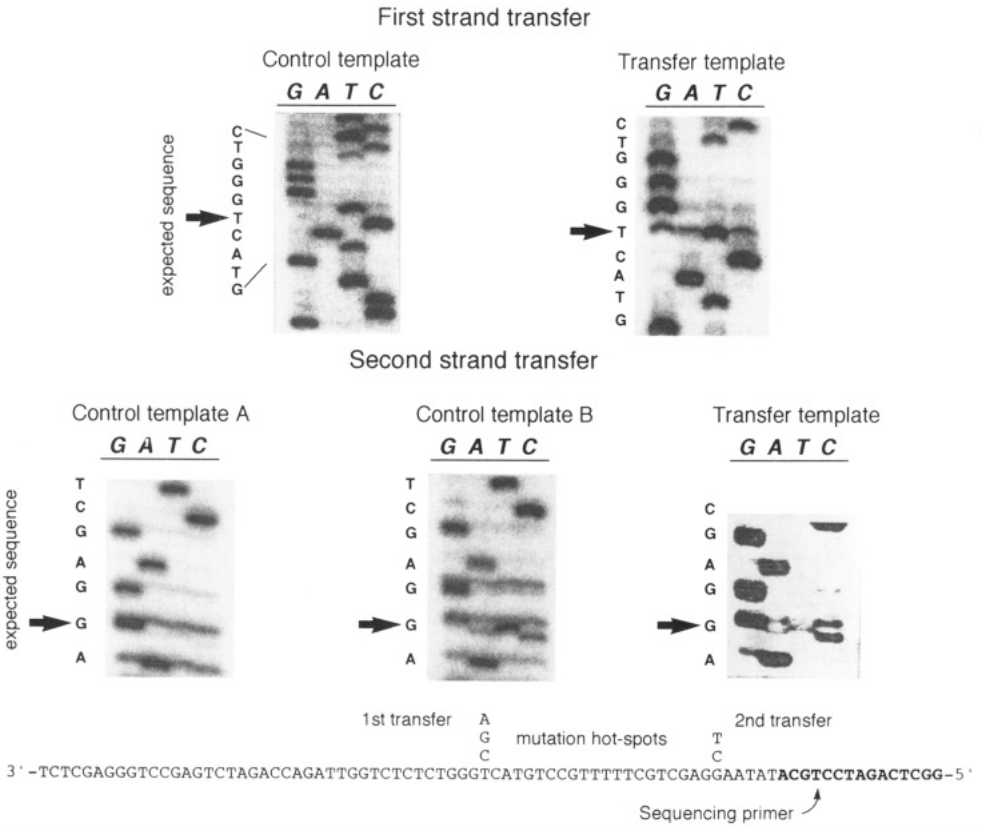

FIGURE 4: Sequence of DNA strand transfer products. Reactions were identical to those described in Figure 3. Strand transfer products were partially purified by phenol/chloroform extraction and Sephadex G-25. The resulting DNA was hybridized to a 5′-^{32}P-labeled 15-base DNA primer (see Figure 2B) and sequenced using the dideoxynucleotide method with modifications for sequencing short DNA templates. The resulting sequences surrounding the first and second strand transfer junctions are shown. The sequences of the control templates A and B are shown for comparison. The expected sequence is shown at the left, and the arrow indicates the expected site of sequence variation predicted by the model in Figure 1B.

Scheme 2

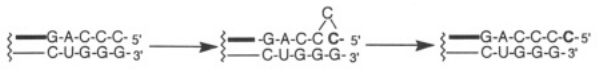

also detected followed by dGMP and dTMP. However, the product resulting from the complete strand transfer reaction shows a different distribution of nucleotides at this site. Under these conditions, little incorporation of dAMP (sequenced as T) or dTMP (sequenced as A) was observed, and dCMP (sequenced as G) is preferentially incorporated during strand transfer. Therefore, factors in addition to the proficiency with which a particular dNMP is incorporated onto the blunt-end intermediate contribute to the misincorporation distribution during the transfer event. It should also be noted that no mutations resulting from addition of more than one nucleotide onto the blunt-end intermediate before transfer were observed, consistent with an earlier observation that these products support strand transfer with much lowered efficiency (Peliska & Benkovic, 1992).

There are several factors which may dictate which bases are incorporated at recombination sites during strand transfer. First, a process involving DNA dislocation (Bebenek et al., 1993) does not appear to influence blunt-end addition during recombination in our model system. If such a process occurred with the RNA templates used here, the first transfer site would have a high occurrence of dCMP incorporation (Scheme 2). While incorporation of dCMP into the strand transfer product was significant, it was not dramatically higher than that observed for dTMP and certainly less than that for dAMP. Also, the observation that dCTP is the *slowest* substrate for blunt-end addition on preformed blunt-end duplexes (Peliska & Benkovic, 1992) suggests that a misalignment mechanism is not a major kinetic determinant of strand transfer fidelity at this site. However, because of the limited resolution of our sequencing protocol, we cannot rule out possible minor contributions of misalignment to the fidelity of strand transfer in this model system. Likewise, at the second transfer site, DNA dislocation at the blunt end would give rise to a high level of dCMP incorporation. The sequence resulting from the 62-base control template (Figure 4) suggests this is not the case since dAMP again is the major observed product (sequenced as T). These results do not rule out the possibility that other sequences may influence the propensity for dislocation at the blunt end. The sequences surrounding the strand transfer sites used in these studies are G-C-rich while dislocation during processive DNA synthesis is typically observed in regions of high A-T content (Bebenek et al., 1989). Further studies are necessary to determine whether such sequences may promote dislocation-mediated blunt-end addition.

Base insertion resulting in a frameshift mutation was not observed. When the sequencing control template A (Figure 4) was run in gel lanes directly adjacent to the transfer template, no upward-shifted band pattern indicative of a frameshift insertion was observed, and all corresponding bands migrated in an identical fashion (not shown). Given the high resolution of the 20% acrylamide gels used in the sequencing, such a shift would have been easily detected. There are, however, "split" bands at the transfer junctions (Figure 4, second jump) that might suggest an insertion in some of the products. However, if this were the case, all the bands above this position would also be split—this is not observed. The

Scheme 3

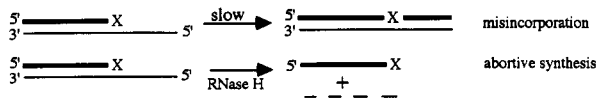

anomalous band pattern at this position is probably due to sequence-dependent changes in electrophoretic mobility[1] and not a frameshift mutation.

The ability of a particular 3′-terminal mismatch to be extended by the polymerase activity of HIV-1 RT (Perrino et al., 1989; Ricchetti & Buc, 1990; Yu & Goodman, 1992) may also play a part in determining misincorporation frequency during strand transfer. If a particular terminal mismatch is formed during strand transfer that is inefficiently extended by HIV-1 RT, the RNase H degradation of the RNA template may compete with DNA extension. Such RNA degradation would result in abortive synthesis since the template can no longer support DNA synthesis (Scheme 3).

Thus, high-frequency blunt-end addition products are not necessarily incorporated into the final strand transfer product in equally high frequency. This is apparently the case during the second strand transfer event described above. While dAMP was efficiently added to the blunt end of the intermediate DNA·RNA duplex, dAMP incorporation during the strand transfer event is much less efficient, suggesting the intermediate A-G mismatch is poorly extended by HIV-1 RT during strand transfer (Figure 4). Thus, even though dCMP from our previous study (Peliska & Benkovic, 1992) is incorporated onto the blunt-end duplex intermediate with lowered efficiency (14-fold) than dAMP, only dCMP (sequenced as G) is prominent in the strand transfer product. In support of this, previous studies have indicated that HIV-1 RT extends pyrimidine-purine mispairs with higher efficiency than purine-purine mispairs (Perrino et al., 1989). Factors including the identity of the mismatch and the sequence surrounding the terminal mismatch may contribute to the overall efficiency of mismatch extension and therefore recombination-induced misincorporation.

These studies do not address the possibility that other core proteins influence the fidelity of DNA strand transfer. Recent studies suggest that reverse transcription may occur within a multiprotein complex (Bowerman et al., 1989; Farnet et al., 1991; Bukrinsky et al., 1993). Also, the viral nucleocapsid protein NCp7 is present in large quantities in the viral core (Darlix et al., 1990). The nucleocapsid protein does appear to influence the kinetics and mechanism of DNA strand transfer reactions *in vitro* (unpublished results). Preliminary results suggest that NCp7 accelerates strand transfer severalfold, but without apparent elimination of blunt-end addition products (unpublished results). Thus, even in the presence of NCp7, recombination fidelity is expected to be low.

A general characteristic of all retroviruses is their high mutation rate, allowing adaptive resistance to a wide range of antiviral drugs. A major source of the genetic instability is probably due to misincorporation errors occurring during reverse transcription (Bebenek & Kunkel, 1993). While the HIV RT alone is capable of misincorporation rates as high as 1 misincorporation per 5000 nucleotides incorporated, the distribution of polymerization errors observed by a variety of methods *in vitro* does not always correlate with those seen *in vivo* (Bebenek & Kunkel, 1993; Boyer et al., 1992; Ji & Loeb, 1992). While RNA nicks in retroviral genomes are commonly observed (Darlix et al., 1977; Coffin, 1979; Meric & Spahr, 1986), the exact degree of fragmentation is not known and could conceivably vary greatly depending on a variety of factors. On the basis of the model presented, the degree to which recombination-induced mutations could contribute to genetic variation would be proportional to the integrity of the viral RNA genome.

ACKNOWLEDGMENT

We thank Dr. Christine Debouck for her generous gift of HIV-1 RT and Kaye Yarnell for her expert assistance in preparing the manuscript.

REFERENCES

Bebenek, K., & Kunkel, T. A. (1993) in *Reverse Transcriptase* (Skalka, A. M., & Goff, S. P., Eds.) p 85, Cold Spring Harbor Laboratory Press, Cold Spring Harbor, NY.
Bebenek, K., Abbotts, J., Roberts, J. D., Wilson, S. H., & Kunkel, T. A. (1989) *J. Biol. Chem. 264*, 16948.
Bowerman, B., Brown, P. O., Bishop, J. M., & Varmus, H. E. (1989) *Genes Dev. 3*, 469.
Boyer, J. C., Bebenek, K., & Kunkel, T. A. (1992) *Proc. Natl. Acad. Sci. U.S.A. 89*, 6919.
Bukrinsky, M. I., Sharova, N., McDonald, T. L., Pushkarskaya, T., Tarpley, W. G., & Stevenson, M. (1993) *Proc. Natl. Acad. Sci. U.S.A. 90*, 6125.
Coffin, J. M. (1979) *J. Gen. Virol. 42*, 1.
Darlix, J.-L., Bromley, P. A., & Spahr, P.-F. (1977) *J. Virol. 23*, 659.
Darlix, J.-L., Gambus, C., Nugeyre, M. J., Clavel, F., & Barre-Sinoussi, F. (1990) *J. Mol. Biol. 216*, 389.
Farnet, C. N., & Hasteltine, W. A. (1991) *J. Virol. 65*, 1910.
Grodberg, J., & Dunn, J. J. (1988) *J. Bacteriol. 170*, 1245.
Hu, W. S., Pathak, V. K., & Temin, H. M. (1993) in *Reverse Transcriptase* (Skalka, A. M., & Goff, S. P., Eds.) pp 251–274, Cold Spring Harbor Laboratory Press, Cold Spring Harbor, NY.
Ji, J., & Loeb, L. A. (1992) *Biochemistry 31*, 954.
Mendelman, L. V., Petruska, J., & Goodman, M. F. (1990) *J. Biol. Chem. 265*, 2338.
Meric, C., & Spahr, P.-F. (1986) *J. Virol. 60*, 450.
Milligan, J. F., & Uhlenbeck, O. C. (1989) *Methods Enzymol. 180*, 51.
Mizrahi, V., Lazarus, G. M., Miles, L. M., Meyer, C. A., & Debouch, C. (1989) *Archm. Biochem. Biophys. 273*, 347.
Peliska, J. A., & Benkovic, S. J. (1992) *Science 258*, 1112.
Perrino, F. W., Preston, B. D., Sandell, L. L., & Loeb, L. A. (1989) *Proc. Natl. Acad. Sci. U.S.A. 86*, 8343.
Preston, B. D., Poiesz, B. J., & Loeb, L. A. (1988) *Science 242*, 1168.
Reardon, J. E., & Miller, W. H. (1990) *J. Biol. Chem. 265*, 20302.
Ricchetti, M., & Buc, H. (1990) *EMBO J. 9*, 1583.
Roberts, J. D., Bebenek, K., & Kunkel, T. A. (1988) *Science 242*, 1121.
Temin, H. M. (1993) *Proc. Natl. Acad. Sci. U.S.A. 90*, 6900.
Yu, H., & Goodman, M. F. (1992) *J. Biol. Chem. 267*, 10888.